



Direct Displacement-Based Design Versus Performance-Based Plastic Design Approaches for Steel Moment-Resisting Frames

Kazem Shakeri¹ · Hamed Dadkhah¹

Received: 7 November 2020 / Accepted: 8 November 2021 / Published online: 6 January 2022
© King Fahd University of Petroleum & Minerals 2021

Abstract

The aim of this study is to compare direct displacement-based design (DDBD) and performance-based plastic design (PBPD) in order to identify more effective design approach for steel moment-resisting frames. To this end, three steel moment-resisting frames with different heights of 4, 8 and 12 stories have been designed using DDBD and PBPD. Although DDBD obtains higher design base shear in comparison with PBPD in high-rise buildings, DDBD leads a lighter structure than PBPD. This is because of significant difference of these design approaches in the design base shear distribution at the height of structure. DDBD approach distributes the base shear such that the design story shear at upper stories is significantly lower. Because of this distribution model, DDBD leads formation of plastic hinges at columns of upper stories, whereas total plastic hinges have been formed at desirable locations in PBPD. To validate the achievement of design performance level, nonlinear time history analysis of steel moment-resisting frames is performed under twenty-two earthquake records. It can be found from the results that PBPD is the efficient design approach for both low-rise and high-rise steel moment frames, whereas the effectiveness of DDBD approach is questioned by increasing the number of stories of structure.

Keywords Performance-based design · Direct displacement-based design · Performance-based plastic design · Steel moment-resisting frame

1 Introduction

A well-designed structure is one that ensures the achievement of desirable and predictable damage level under design earthquakes. To this end, the behavior of structures in elastic and inelastic ranges should be modeled accurately, whereas current seismic design codes are generally based on elastic analysis and the inelastic behavior is taken into account in a somewhat indirect manner without high accuracy.

In the current US seismic design practice [1] which is a force-based design approach, either the equivalent lateral force method or the modal response spectrum method is used to design the structures. In these methods assuming the elastic behavior for structure, the seismic design base shear is determined from elastic design spectral acceleration and reduced by a response modification factor, R , which is depending on the ductility capacity of the structural system. The seismic

design force is also adjusted according to the importance of structure by an occupancy importance factor, I . After the elastic analysis of structure and the design of structural members, the determined inter-story drift is multiplied by a deflection amplification factor, C_d , in order to estimate the actual inter-story drift including elastic and inelastic drifts. So it can be concluded that the force-based design method has a number of drawbacks as presented in previous researches [2, 3] and no explicit and accurate checks are conducted to determine ultimate strength and deformations. The force distribution according to elastic analysis, using a force-reduction factor representing the ductility without explicitly evaluation of ductility demands, and the estimation of inter-story drift from the elastic inter-story drift are the main drawbacks of the force-based design method. To overcome these drawbacks, performance-based design approach has been proposed that its main goal is to achieve a desirable performance level under a specific level of earthquake.

The performance-based design is capable of predicting the seismic behavior of structure with a high accuracy because of the inelastic analysis. This method is an acceptable design approach for satisfying the desires of the structure's own-

✉ Kazem Shakeri
shakeri@uma.ac.ir

¹ Department of Civil Engineering, Faculty of Engineering, University of Mohaghegh Ardabili, Ardabil, Iran



ers. The performance-based design framework has been first proposed to evaluate and retrofit the seismic performance of existing structures [4]. However, this method can be also carried out for the design of structure by performing a series of designs and evaluations in an iterative manner. This iterative design approach causes a high computational cost and time and also, an initial good design is necessary to achieve the desired performance level after iteration [5]. The next-generation performance-based seismic design has been developed based on probabilistic approach in FEMA P-58 [6]. This guideline is also a probabilistic evaluation criteria and does not present a direct design method. However, in recent years, researchers have focused on integrating the mean annual frequency of collapse and expected monetary losses into the design process [7, 8].

Recently different performance-based design approaches, such as the yielding point spectra method [9], the modified lateral force procedure [10], the direct displacement-based design (DDBD) and the performance-based plastic design (PBPD), have been developed to design the structural systems without the requirement of iteration in the design process. In these methods, inelastic behavior of structure is directly taken into account to determine the seismic design force. The most developed performance-based design approaches are DDBD and PBPD methods.

DDBD is one of the more popular performance-based design approaches which has been developed by Priestley [2]. This method has been also published as a text by Priestley et al. [3] and in a model-code format [11]. In the DDBD, the structures are designed to achieve inter-story drift corresponding to a specified performance level. To this end, the multi-degree of freedom (MDOF) structure is replaced by the equivalent linearized single degree of freedom (SDOF) system. The dynamical properties of this substitute SDOF system are determined by selecting an inelastic mode shape for the structure. The substitute structure mythology had been first proposed by Shibata and Sozen [12] for RC structures. Because the effective period of the substitute SDOF system and the seismic design force are determined using an elastic displacement response spectrum, the inelastic behavior and hysteretic damping of structure is simulated by an equivalent damping. Sullivan [13] studied the highlighting differences between force-based design and DDBD for RC frame structure and showed that the design base shear of DDBD is one half to four times that of force-based design. The DDBD has been extensively developed and tested for different RC structural systems [14–16]. Medhekar and Kennedy [17] first developed this method for an eight-story steel frame having concentrically braced system. The DDBD has been employed to design different steel frame structures, such as concentrically braced frame structures [18–20], eccentrically braced frame structures [21–23], and steel moment-resisting frames [24, 25]. Roldán et al.

[25] developed DDBD approach for steel moment-resisting frames, while the flexibility of beam-to-column connections joints has been considered in the design process. Different structural control systems have been also designed using this method [26–29]. These researches show the effectiveness of the DDBD in reliably meeting the desirable performance level. O'Reilly and Calvi [30] also studied how structures designed using DDBD may be verified in a risk-consistent manner using demand-intensity models. However in the some researches [24, 31], it has been shown that the considered limitation on the inter-story drift has been not satisfied effectively.

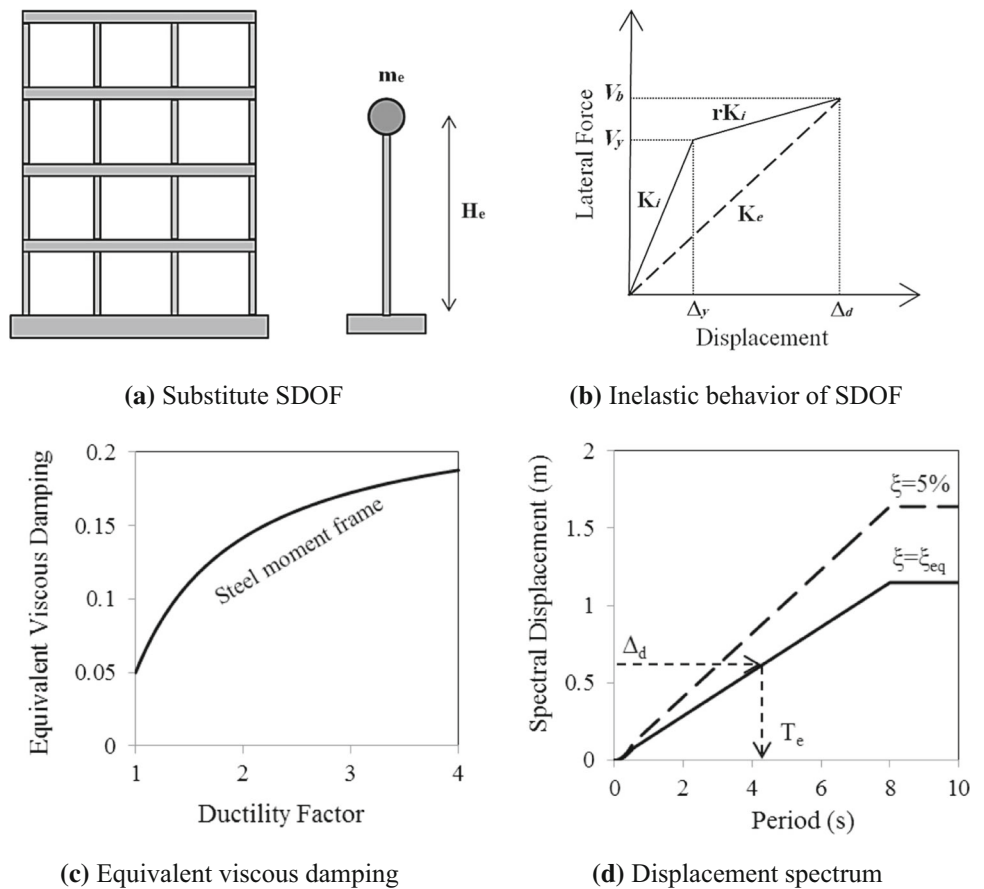
PBPD is another effective design approach which has recently received notable acceptance among researchers. This method had been first proposed by Leelataviwat et al. [32] and then developed by different researchers [33, 34]. Similar to DDBD, PBPD directly considers inelastic structural behavior in the design process and practically requires no iteration after initial design. In this method, assuming a target inter-story drift and a desirable yield mechanism, the seismic design force is determined based on the concept of energy balance. This concept in a simple form had been first used by Housner [35] for the design of structure. The PBPD has been extensively developed and employed to design different structural systems, such as steel moment-resisting frame [36–38], eccentrically braced steel frame [39], concentrically braced steel frame [40], buckling restrained braced frame [41], and special truss moment frame [42]. It can be found from these researches that PBPD is effectiveness in the achievement of target inter-story drift under design earthquakes.

Although DDBD and PBPD approaches have been proposed for the same goal that is to achieve a target inter-story drift under design earthquakes, these methods are based on totally different concepts. The aim of this study is to compare these design approaches to identify more effective approach. To this end, steel moment-resisting frames are designed using DDBD and PBPD methods and a comparison between the design results is conducted. In order to identify more effective design approach, the nonlinear time history analysis of designed frames is performed under twenty-two earthquake records suggested by FEMA P695 [43].

2 Direct Displacement-Based Design Approach

The fundamental of DDBD has been explained in more detail in previous publications [3, 14], and only a brief review is presented here. As noted, the basic of DDBD is replacing the MDOF structure with a substitute SDOF system as shown in Fig. 1a. The bilinear force–displacement behavior of the substitute SDOF system is presented in Fig. 1b,

Fig. 1 Fundamental of DDBD approach



where K_e is the secant stiffness at maximum displacement Δ_d which is determined based on the design displacement of the structure. Other characteristics of SDOF system, such as maximum the effective mass M_e and the effective height H_e , are also determined based on this design displacement. In order to use the elastic displacement spectrum in the design process, the bilinear behavior of SDOF system should be represented by an equivalent linearized SDOF system. To this end, the dissipated energy during inelastic response is equalized with a viscous damping and a relationship between the expected ductility demand and the equivalent viscous damping is defined as shown in Fig. 1c for steel moment-resisting frame. According to the maximum displacement Δ_d and the equivalent viscous damping, the effective period T_e can be determined from the elastic displacement spectrum specified for different level of damping as shown in Fig. 1d. Finally, the effective stiffness K_e at the maximum displacement and the design base shear can be found based on the effective period T_e .

Priestley et al. [3] proposed that when the stability index is less than 0.085, P-Delta effect may be ignored. The stability index of archetype buildings of this study is less than this value, so P-Delta effect has not been considered to avoid more complexity. According to the mentioned points, the design

steps of DDBD can be classified for steel moment-resisting frames as follow:

Step 1: The first step of designing each building structure is determining a target inter-story drift corresponding to the considered performance level. In this study, the achievement of life safety performance level under seismic hazard having a probability of occurrence 10% in 50 years has been defined as design objective. The Vision 2000 [44] proposes the inter-story drift ratio to be equal to 1.5% for life safety, while the corresponding value has been considered as 2.5% for steel moment frames in FEMA 356 [4]. In the model-code format of DDBD [11] as well as previous researches [24, 45], the inter-story drift limit of 2.5% has been specified for steel moment frames. Hence in this study, 2.5% is defined as target inter-story drift ratio for life safety performance level.

Step 2: In this step, the design displacement shape of structure is determined based on a mode shape and target inter-story drift. If the drift limit is defined so that the behavior of structure remains elastic range, the elastic first mode shape can be taken as design mode shape, while the structure will experience inelastic behavior in the inter-story drift of 2.5%. Hence, the assumed mode shape should be included both elastic and inelastic responses structure. In previous researches of DDBD, different empirical mode shapes have

been used to determine the design displacement shape [3, 46]. In this study, the following equations are used as mode shape which Pettinga and Priestley [46] showed to be appropriate for the design process of regular frame buildings:

$$\text{for } n \leq 4 : \delta_i = H_i / H_n \quad (1a)$$

$$\text{for } n > 4 : \delta_i = \frac{4}{3} \left(\frac{H_i}{H_n} \right) \left(1 - \frac{H_i}{4H_n} \right) \quad (1b)$$

where δ_i is the inelastic mode shape, n is the number of stories of structure, and H_i and H_n are, respectively, the heights of level i and roof. According to this mode shape and the target displacement Δ_c , the design displacement shape is determined as follows:

$$\Delta_i = \delta_i \left(\frac{\Delta_c}{\delta_c} \right) \quad (2)$$

where δ_c is the value of shape mode at the critical level that causes the greatest inter-story drift according to the mode shape. From the considered mode shape, first story is the critical level. Equation (2) is the design displacement shape presented in Priestley et al. [3]. This study uses this equation as the design displacement shape. The design displacement shape presented in DBD12 model code [11], which integrates Eqs. (1) and (2), can be also used.

Step 3: Determine the design displacement Δ_d according to Eq. (3).

$$\Delta_d = \sum_{i=1}^n m_i \Delta_i^2 / \sum_{i=1}^n m_i \Delta_i \quad (3)$$

where m_i the seismic mass at the level i .

Step 4: Calculate the effective mass of the substitute SDOF system m_e according to Eq. (4).

$$m_e = \sum_{i=1}^n m_i \Delta_i / \Delta_d \quad (4)$$

Step 5: Determine the yield displacement of structure Δ_y according to Eq. (5).

$$\Delta_y = \theta_y H_e \quad (5)$$

where H_e is the effective height of substitute SDOF system which is determined as follows:

$$H_e = \sum_{i=1}^n m_i \Delta_i H_i / \sum_{i=1}^n m_i \Delta_i \quad (6)$$

and θ_y is the yield drift ratio given by Eq. (7) for structural steel frames [3].

$$\theta_y = 0.65 \varepsilon_y L_b / h_b \quad (7)$$

where ε_y is the yield strain of steel, L_b and h_b are the beam span and the beam depth, respectively. Priestley et al. [3] proposed Eq. (7) for steel moment-resisting frames with full-strength joints. For other types of beam-to-column joints with semi-rigid and partial strength, the yield drift ratio can be found in Roldán et al. [25].

Step 6: The design ductility factor μ is determined as follows:

$$\mu = \Delta_d / \Delta_y \quad (8)$$

Step 7: Determine the equivalent viscous damping including the elastic damping and the hysteretic damping.

The key point of DDBD is to simulate the dissipated energy during inelastic response with an equivalent viscous damping. In the simplest method, the relationships have been proposed based on the area of a hysteretic loop by using Jacobsen's equivalent damping approach [47]. This approach has been suggested for harmonic motion, whereas the earthquake excitation applied to the structure is not harmonic. Hence, the equivalent damping ratio determined by this approach was overestimated [48], and in previous researches [49, 50], several modifications have been proposed to derive the equivalent damping that in these researches, the equivalent viscous damping was varied until the results of the linearized substitute structure matched that of the inelastic model. Priestley et al. [3] showed that the result of area-based equivalent damping approach is incompatible with that of inelastic time history analyses and proposed the correction factors for different hysteresis rules. In this study, the equivalent viscous damping ξ_{eq} is determined according the relationship proposed by Priestley et al. [3] as follows:

$$\xi_{eq} = 0.05 + C \left(\frac{\mu - 1}{\mu \pi} \right) \quad (9)$$

where C is a coefficient depending on the hysteresis rule of structure which $C = 0.577$ has been proposed for steel frame building.

Step 8: Scale the elastic displacement spectrum down to the expected equivalent viscous damping level.

To this end, different scale factors can be found in previous researches [51–53]. In this study, the scale factor recommended by Eurocode 8 [53] is employed as follows:

$$R_\xi = \left(\frac{0.1}{0.05 + \xi_{eq}} \right)^{0.5} \quad (10)$$

Step 9: Determine the effective period T_e from the scaled displacement spectrum for the design displacement Δ_d as shown in Fig. 1d.

Step 10: Determine the effective stiffness K_e and the design base shear V_b as follows:

$$K_e = \frac{4\pi^2 m_e}{T_e^2} \tag{11}$$

$$V_b = K_e \Delta_d \tag{12}$$

Step 11: Analysis of structure under the design base shear.

To this end, the design base shear should be first distributed to each level based on the design displacement shape using:

$$F_i = \frac{m_i \Delta_i}{\sum_{i=1}^n m_i \Delta_i} V_b \tag{13}$$

where F_i is the design force applied on the level i .

For analysis of structure under distributed design base shear, the equilibrium-based analysis method recommended by Priestley et al. [3] is employed. In this method which in more detail can be found in Priestley et al. [3], the sum of beam shear forces V_{B1i} is derived for exterior span of a three-span frame as follows:

$$\sum_{i=1}^n V_{B1i} = T = \frac{M_1}{2M_1 + M_2} \left(\sum_{i=1}^n F_i H_i - \sum_{j=1}^m M_{Cj} \right) / L_1 \tag{14}$$

where T is the seismic axial force of columns, M_1 and M_2 are, respectively, the design moments of exterior and interior spans, L_1 is the length of exterior span, and m and M_{Cj} are, respectively, the number and moment of columns at the base. For more clarity, the free-body diagram is presented in Fig. 2. Assuming the point of contra-flexure at 60% of story height in the first story, the column base moments is given by:

$$\sum_{j=1}^m M_{Cj} = 0.6V_b H_1 \tag{15}$$

where H_1 is the first story height. Similarly the sum of beam shear forces V_{B2i} for interior span is determined as:

$$\sum_{i=1}^n V_{B2i} = T = \frac{M_2}{2M_1 + M_2} \left(\sum_{i=1}^n F_i H_i - \sum_{j=1}^m M_{Cj} \right) / L_2 \tag{16}$$

where L_2 is the length of interior span. To determine the beam shear force at each level, the sum of beam shear forces

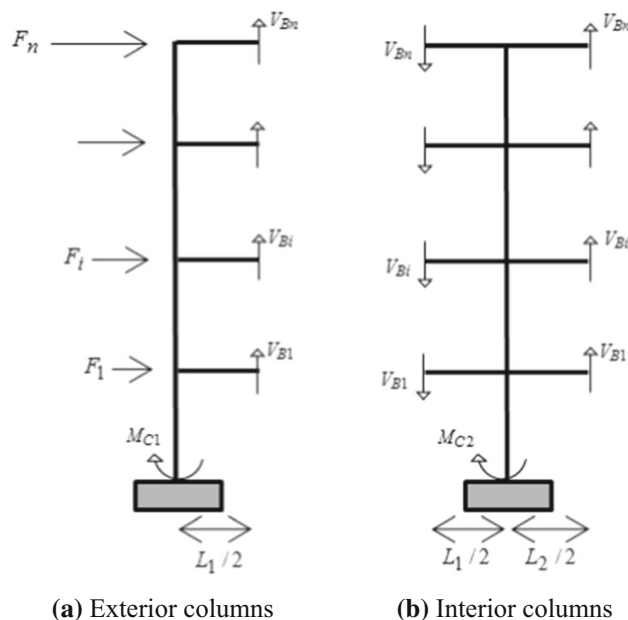


Fig. 2 Free-body diagram of columns in DDBD approach

should be distributed that Priestley et al. [3] recommended a distribution according to the story shear force as follows:

$$V_{Bi} = T \frac{V_{S,i}}{\sum_{i=1}^n V_{S,i}} \tag{17}$$

where V_{Bi} is the beam shear force at level i and $V_{S,i}$ is the story shear force of level i determined as:

$$V_{S,i} = \sum_{k=1}^n F_k \tag{18}$$

Step 12: Design of beam members.

The design of frame members is conducted based on the moment demand and regardless of shear and axial demands. The requirement for capacity design of beams can be defined by

$$\varphi_s M_{DB} > M_{EB} \tag{19}$$

where φ_s is the strength-reduction factor and M_{EB} is the required design moment of beam which at level i , is determined by

$$M_{EB,i} = V_{Bi}(L - h_c)/2 \tag{20}$$

where L and h_c are the length of each span and the column depth, respectively.

Step 13: Capacity design of columns. The design of beam members

For capacity design of columns, the general requirement is defined as follows:

$$\varphi_s M_{DC} > \varphi^o \omega M_{EC} \quad (21)$$

where φ^o is the ratio of overstrength moment capacity to required capacity which is different for steel sections [54]. From AISC 341–10 [55], this ratio can be considered as $1.1R_y$ where R_y is the ratio of expected yield stress to the specified minimum yield stress. ω is a dynamic amplification factor due to higher mode effects where from the first story to the $\frac{3}{4}$ of structure height is given by [3]

$$\omega = 1.15 + 0.13(\mu^o - 1) \quad (22a)$$

$$\mu^o = \mu / \varphi^o \geq 1 \quad (22b)$$

and for other stories of structure, is reduced linearly in a way that this factor is $\omega = 1$ at the top of structure. M_{EC} is the required column design moment which has been recommended to be determined based on the strong column-weak beam design criterion [3]. Hence, for exterior columns in a one-way frame at level i , the required column design moment is determined by Eq. (23), while for interior columns, the moment will be twice this.

$$M_{EC,i} = M_{EB,i}/2 \quad \text{for } i = 1, 2, \dots, n - 1 \quad (23a)$$

$$M_{EC,i} = M_{EB,i} \quad \text{for } i = n \quad (23b)$$

In Eq. (21), the effect of axial force has not been considered in this case study, because its effect is negligible. The demand/capacity ratio related to axial force is less than 0.05 for the lateral resisting frames designed in this study. This low ratio is due to that the gravity-bearing area of lateral resisting frame is significantly less than its seismic-bearing area. The effect of gravity force has been also considered in combination with seismic force for this reason.

3 Performance-Based Plastic Design Approach

As noted earlier, PBPD is developed based on the concept of energy balance and uses a target inter-story drift and a desirable yield mechanism as design objective. In this method, the work needed to push the structure monotonically up to the target drift (Fig. 3a) is equated to the energy required by an equivalent elastic–plastic SDOF system (Fig. 3b) to drive the design base shear force.

As shown in Fig. 3a, a distribution of lateral design force should be assumed to push the structure according to this distribution. A distribution based on inelastic dynamic response

results [33, 56], which has been recommended by Goel and Chao [57] for the PBPD, is used as follows:

$$F_i = C_i V_y \quad (24a)$$

$$C_i = (\beta_i - \beta_{i+1}) \left(\frac{m_n H_n}{\sum_{j=1}^n m_j H_j} \right)^{0.75T^{-0.2}} \quad (24b)$$

$$\beta_i = \frac{V_i}{V_n} = \left(\frac{\sum_{j=i}^n m_j H_j}{m_n H_n} \right)^{0.75T^{-0.2}} \quad (24c)$$

where V_y is the required design base shear; β_i is the shear distribution factor at level i , T is the fundamental period of structure, and V_i and V_n are the story shears at levels of i and the top of structure. Chao et al. [56] showed that this distribution leads to more realistic story shear as well as uniform inter-story drifts over the structure height.

Assuming an idealized elastic–plastic force–deformation behavior, the work–energy equation can be written as:

$$E_e + E_p = \gamma \left(\frac{1}{2} M S_v^2 \right) = \frac{1}{2} \gamma M \left(\frac{T}{2\pi} S_{ag} \right)^2 \quad (25)$$

where E_e and E_p are the elastic and plastic energies of structure to push it up to the target inter-story drift, respectively; M is the total mass of system; S_v and S_a are the design pseudo-spectral velocity and the design pseudo-spectral acceleration, respectively; γ is the energy modification factor which can be determined by using the geometric relationship between the two areas representing work and energy shown in Fig. 3b as follows:

$$\frac{1}{2} V_y (2\Delta_u - \Delta_y) = \gamma \left(\frac{1}{2} V_e \Delta_{eu} \right) \quad (26)$$

The parameters defined in Eq. (26) are shown in Fig. 3b. This equation can be written in the reduced form as follows:

$$\gamma \frac{\Delta_{eu}}{\Delta_y} = \frac{2\Delta_u - \Delta_y}{\Delta_{eu}} \quad (27)$$

Finally, the energy modification factor can be obtained by the following relationship:

$$\gamma = \frac{2\mu_s - 1}{R_\mu^2} \quad (28)$$

As shown, the energy modification factor is depending on the structural ductility factor, μ_s , and the ductility reduction

Fig. 3 Fundamental of PBPD approach

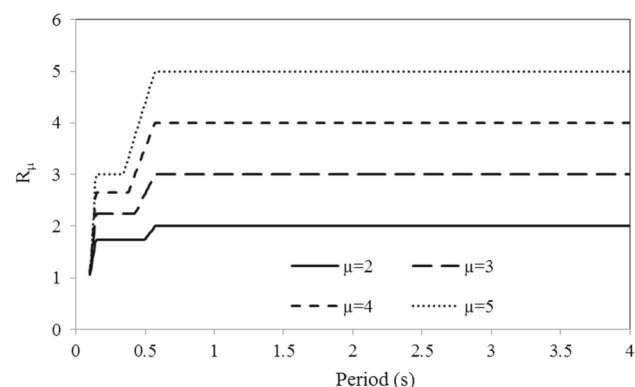
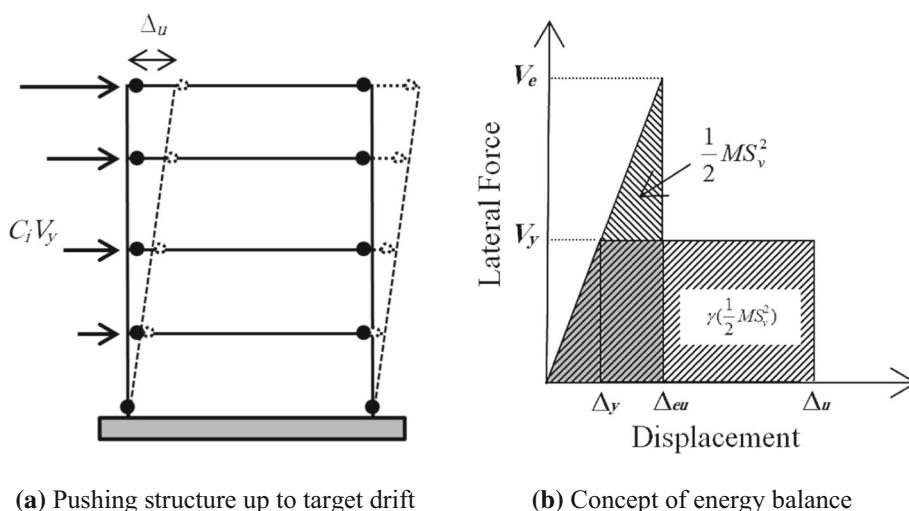


Fig. 4 Elastic-plastic spectrum proposed by Newmark and Hall [51]

factor, R_{μ} . μ_s can be determined based on the target inter-story drift and assuming a yield drift, and R_{μ} can be also defined as function of μ_s according to inelastic spectrums of elastic-plastic SDOF system. The spectrum proposed by Newmark and Hall [51] is used to relate R_{μ} and μ_s as shown in Fig. 4. This figure has been developed with respect to the initial stiffness of the system, whereas the DDBD uses the secant stiffness to determine the design base shear force.

Akiyama (1985) showed that the elastic energy can be determined by assuming that the structure is reduced into a SDOS system as follows:

$$E_e = \frac{1}{2} M \left(\frac{T}{2\pi} \cdot \frac{V_y}{W} g \right)^2 \tag{29}$$

On the other hand, assuming a desirable yield mechanism as shown in Fig. 3a and equating the plastic energy to the work done by design lateral forces, the work energy equation can be rewritten as follows:

$$\frac{1}{2} \frac{W}{g} \left(\frac{T}{2\pi} \cdot \frac{V_y}{W} g \right)^2 + V_y \left(\sum_{i=1}^n C_i H_i \right) \theta_p = \frac{1}{2} \gamma \frac{W}{g} \left(\frac{T}{2\pi} S_a g \right)^2 \tag{30}$$

where θ_p is the plastic component of the target drift ratio. From Eq. (30), the required design base shear is determined as:

$$\frac{V_y}{W} = \frac{-\alpha + \sqrt{\alpha^2 + 4\gamma S_a^2}}{2} \tag{31}$$

where α is a dimensionless parameter given by

$$\alpha = \left(\sum_{i=1}^n C_i H_i \right) \cdot \left(\frac{\theta_p 8\pi^2}{T^2 g} \right) = \left(\sum_{i=1}^n (\beta_i - \beta_{i+1}) H_i \right) \cdot \left(\frac{m_n H_n}{\sum_{j=1}^n m_j H_j} \right)^{0.75T-0.2} \cdot \left(\frac{\theta_p 8\pi^2}{T^2 g} \right) \tag{32}$$

According to the mentioned points, the design steps of PBPD can be classified for steel moment-resisting frames as follow:

Step 1: Determine a target inter-story drift corresponding to the considered performance level. As noted in previous section, 2.5% is defined as target drift ratio, θ_u , for life safety performance level.

Step 2: Assume a yield drift ratio θ_y . As recommended by Goel and Chao [57], 1% is considered as the yield drift ratio of moment frames.

Step 3: Calculate the structural ductility factor according to Eq. (33).

$$\mu = \frac{\theta_u}{\theta_y} \tag{33}$$

Step 4: Estimate the fundamental period of structure. To this end, the following equation proposed by ASCE 7–10 [1] is used.

$$T = 0.0724H_n^{0.8} \tag{34}$$

Step 5: Determine the ductility reduction factor R_μ . According to the inelastic spectrum proposed by Newmark and Hall [51], R_μ is determined by the following equation because the fundamental period of structures considered in this study is more than 0.57 s.

$$R_\mu = \mu \tag{35}$$

Step 6: Determine the energy modification factor according to Eq. (28).

Step 7: Calculate the dimensionless parameter α from Eq. (32) where $\theta_p = \theta_u - \theta_y$.

Step 8: Determine S_a from the elastic design spectra for the estimated fundamental period of structure.

Step 9: Calculate the design base shear force from Eq. (31).

Step 10: Distribute the design base shear force to each level according to Eq. (24).

Step 11: Plastic design of beams [57]

To this end, the required plastic moment of base columns is first derived by using the condition that no soft story mechanism would occur in the first story. In this regard, a 10% increase is considered in the design base shear due to overstrength. Thus,

$$M_{pc} = \frac{1.1V_y H_1}{4n_s} \tag{36}$$

where M_{pc} is the required plastic moment at the base and n_s is the number of bays.

Then, the required plastic moment of beam at each level is determined using plastic design approach referring to Fig. 5:

$$\sum_{i=1}^n F_i H_i \theta_p = 2M_{pc} \theta_p + \sum_{i=1}^n 2(\beta_i M_{pb}) \gamma_i \tag{37}$$

where M_{pb} and $\beta_i M_{pb}$ are the required moment strengths of beam at the top floor level and level i , respectively; $\gamma_i = (L/L'_i)\theta_p$ is the rotation term as shown in Fig. 5. In this study, it is assumed that L/L'_i is 0.8375. By solving Eq. (37), the required moment strength of beam at level i , $M_{pb,i} = \beta_i M_{pb}$

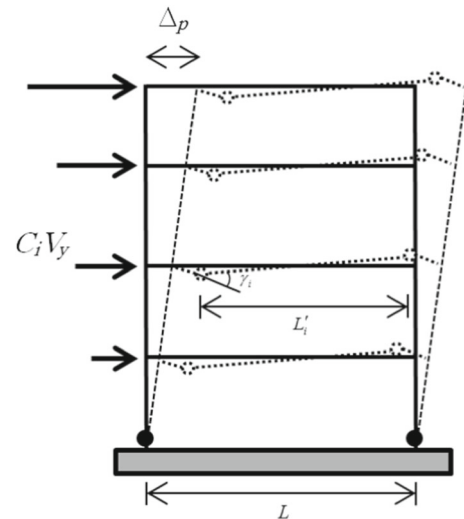


Fig. 5 Yield mechanism of steel moment frame in PBPD approach

can be determined. Finally, the required design moment of beam is determined as follows:

$$\phi_s M_{DB,i} > M_{pb,i} \tag{38}$$

Step 12: Design of exterior columns

To this end, an equilibrium approach is used for the free-body diagram of exterior columns as shown in Fig. 6a. The columns of moment frame, which are not designed to yield, must be designed for the maximum expected forces by considering a reasonable extent of strain-hardening and material overstrength in the beam plastic hinges. The columns at the base are assumed to have reached their maximum capacity, M_{pc} , and the moment at a strain-hardened beam plastic hinge, M_{pr} , is determined by the following equation.

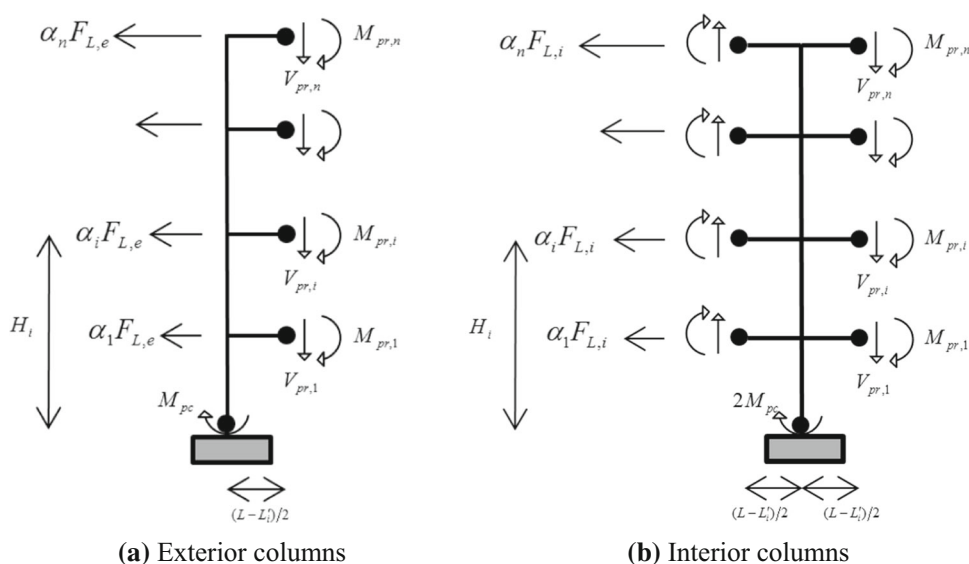
$$M_{pr,i} = C_{pr} R_y M_{pb,i} \tag{39}$$

where C_{pr} and R_y are coefficients representing the effects of strain-hardening and material overstrength, respectively. Goel and Chao [57] recommended $C_{pr} = 1$ for the beams of top story and $C_{pr} = 1.075$ for other stories. The value of beam shear at a plastic hinge, V_{pr} , can be also determined as follows:

$$V_{pr,i} = \frac{2M_{pr,i}}{L'} \tag{40}$$

The lateral force applied on exterior columns can be determined by assuming that its distribution is the same as Eq. (24)

Fig. 6 Free-body diagram of columns in PBDP approach



and equating the moment equilibrium in the free-body diagram shown in Fig. 6a as follows:

$$F_{L,e} = \frac{\sum_{i=1}^n M_{pr,i} + \sum_{i=1}^n V_{pr,i}(L - L'_i)/2 + M_{pc}}{\sum_{i=1}^n \alpha_i H_i} \tag{41a}$$

$$\alpha_i = \frac{\beta_i - \beta_{i+1}}{\sum_{i=1}^n (\beta_i - \beta_{i+1})} \tag{41b}$$

Finally, the required design moment of exterior columns at each level can be simply determined from the equilibrium equations.

Step 13: Design of interior columns

The required design moment of interior columns is obtained in the same approach as previous step. The only difference is in the lateral force applied on interior columns which is determined by the following equation according to the moment equilibrium in the free-body diagram shown in Fig. 6b.

$$F_{L,i} = \frac{2 \sum_{i=1}^n M_{pr,i} + 2 \sum_{i=1}^n V_{pr,i}(L - L'_i)/2 + 2M_{pc}}{\sum_{i=1}^n \alpha_i H_i} \tag{42}$$

In the other words, the lateral force of interior columns is twice that of exterior columns. Hence, it can be concluded that the required design moment of interior columns at each level is twice that of exterior columns.

A peer-to-peer comparison of design methods is performed for more clarity. Their significant differences can be classified as follows:

- (1) DDBD has been developed based on replacing the MDOF structure with a substitute SDOF system, whereas PBDP uses the concept of energy balance in the design process.
- (2) Distribution of lateral design force at the height of building is quite different in DDBD and PBDP.
- (3) PBDP uses the elastic–plastic spectrum in the design process, whereas DDBD defines an equivalent viscous damping in order to be able to simulate the bilinear behavior and DDBD uses the elastic spectrum to find the design shear force.
- (4) PBDP determines the ductility factor based on the target inter-story drift and the number of stories has no effect on the ductility factor. In DDBD, the ductility factor will be different with changing the number of stories.
- (5) PBDP analyzes and designs the structural members using the plastic design concept, whereas DDBD uses the equilibrium-based analysis method for the design of structural members.

4 Archetype Steel Buildings

As noted earlier, the main goal of this study is to compare DDBD and PBDP approaches. To this end, three archetype office buildings with different heights of 4, 8 and 12 stories are designed according to these design approaches. Details

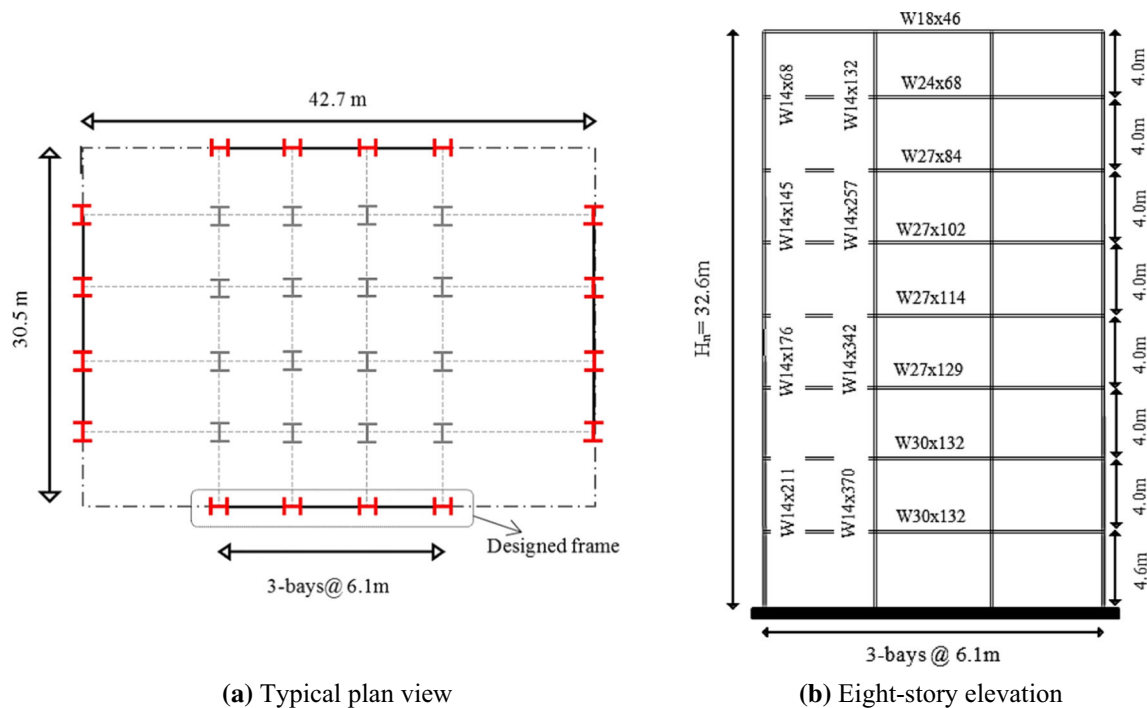


Fig. 7 Archetype building

about these archetype buildings can be found in previous researches [58, 59]. A typical story plan view of the archetype building and an elevation of moment frame are shown in Fig. 7. The buildings have a typical story height of 4 m and a first-story height of 4.6 m. The structural elements including beams and columns are fabricated from steel ASTM A992 Gr. 50 with the yield stress of 345 MPa. It is assumed that the archetype buildings have been located in Los Angeles (site coordinates 34°N, 118°W; seismic design category D; site class D).

5 Performance-Based Design of Archetype Buildings

To identify more effective design approach, the archetype buildings are first designed by DDBD and PBPD, and the nonlinear time history analysis is then performed. In this section, the archetype buildings are designed by using design approaches of DDBD and PBPD and a comparison between the design parameters is performed. The design process of DDBD and its results have been validated with the results of Sullivan and Lago [45]. The implementation of PBPD has been also validated with Goel and Chao [57]. It is noted that the design objective is the achievement of life safety performance level under seismic hazard having a probability of occurrence 10% in 50 years. The elastic design spectrum for this level of seismic hazard is derived from ASCE 7–10 [1]

as presented in Fig. 8. The design spectrum has been determined using the ground motion parameters obtained from the US Seismic Design Maps Web Application. The inputs of this application are the site coordinates (34°N, 118°W), the site soil classification (site class D) and the risk category (I, II or III).

5.1 Archetype Buildings Designed by DDBD

The design process of DDBD explained in Sect. 2 is implemented for the design of archetype buildings. All necessary calculations for the implementation of design steps are presented in Table 1 for twelve-story frame as instance. According to the results presented in Table 1, the design parameter can be simply determined that its results are reported in Table 2. A significant difference can be found between the design base shear of four-story frame with that of others. This is due to a significant difference between the ductility factors of four-story frame and others. As presented in Table 2, the ductility factor of four-story frame is equal to 2.56, whereas the corresponding value is 2.14 and 2.12 for eight and twelve-story frames, respectively. It will be shown in the next section that PBPD assumes the same ductility factor for archetype buildings, so the significant difference cannot be found between the design base shears of archetype buildings in PBPD approach.

The archetype buildings have been analyzed under the design base shear force and the required moment strength

Table 1 Calculations for the design of twelve-story frame with DDBD

	H_i (m)	m_i (ton)	δ_i	Δ_i (m)	$m_i \Delta_i$	$m_i \Delta_i^2$	$m_i \Delta_i H_i$
Story 1	4.6	341.7	0.123	0.115	39.30	4.52	180.76
Story 2	8.6	339	0.226	0.210	71.35	15.02	613.60
Story 3	12.6	339	0.323	0.302	102.28	30.86	1288.78
Story 4	16.6	339	0.416	0.389	131.79	51.23	2187.72
Story 5	20.6	339	0.505	0.471	159.87	75.39	3293.27
Story 6	24.6	339	0.589	0.550	186.52	102.62	4588.30
Story 7	28.6	339	0.669	0.624	211.74	132.25	6055.64
Story 8	32.6	339	0.744	0.694	235.53	163.64	7678.16
Story 9	36.6	339	0.815	0.761	257.89	196.18	9438.71
Story 10	40.6	339	0.881	0.822	278.82	229.32	11,320.14
Story 11	44.6	339	0.943	0.880	298.32	262.53	13,305.31
Story 12	48.6	311.65	1	0.933	290.87	271.48	14,136.47
Σ	–	4043.35	–	–	2264.27	1535.05	74,086.86

Table 2 Design parameters of DDBD

Design parameters	4-Story	8-Story	12-Story
Δ_d (m)	0.309	0.467	0.678
m_e (ton)	1128.49	2266.62	3339.91
H_e (m)	12.35	22.35	32.72
Δ_y (m)	0.12	0.22	0.32
μ	2.56	2.14	2.12
ξ_{eq}	0.162	0.148	0.147
R_ξ	0.687	0.711	0.712
T_e (s)	2.192	3.204	4.642
K_e (MN/m)	9.275	8.719	6.117
V_b (MN)	2.863	4.071	4.147

of structural members has been determined. The design section of structural members has been selected based on this

required moment strength that its results are presented in Table 3.

5.2 Archetype Buildings Designed by PBPD

In this section, the archetype buildings are designed by using PBPD approach presented in Sect. 3. The design process is explained for twelve-story frame in more detail, while it is quite similar for other archetype buildings. For twelve-story frame, the fundamental period of structure from Eq. (34) is 1.618 s where H_n is 48 m. The design pseudo-spectral acceleration for this fundamental period is 0.51 g from the design spectrum shown in Fig. 8. All necessary calculations for determining design parameters are presented in Table 4.

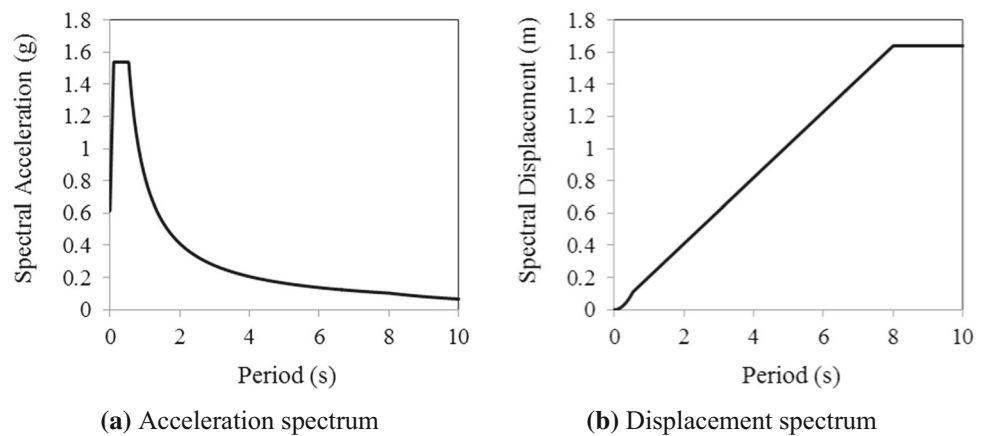
From Table 4 and Eq. (32), the dimensionless parameter is determined as:

Table 3 Archetype buildings designed by DDBD

Story	Twelve-story archetype building			Eight-story archetype building			Four-story archetype building		
	Beams	Exterior columns	Interior columns	Beams	Exterior columns	Interior columns	Beams	Exterior columns	Interior columns
1	W33 × 130	W14 × 211	W14 × 398	W30 × 132	W14 × 211	W14 × 370	W24 × 103	W14 × 145	W14 × 283
2	W33 × 130	W14 × 211	W14 × 398	W30 × 132	W14 × 211	W14 × 370	W24 × 94	W14 × 145	W14 × 283
3	W30 × 132	W14 × 193	W14 × 370	W27 × 129	W14 × 176	W14 × 342	W21 × 83	W14 × 90	W14 × 159
4	W30 × 132	W14 × 193	W14 × 370	W27 × 114	W14 × 176	W14 × 342	W21 × 50	W14 × 90	W14 × 159
5	W30 × 124	W14 × 176	W14 × 342	W27 × 102	W14 × 145	W14 × 257	–	–	–
6	W30 × 116	W14 × 176	W14 × 342	W27 × 84	W14 × 145	W14 × 257	–	–	–
7	W24 × 117	W14 × 145	W14 × 283	W24 × 68	W14 × 68	W14 × 132	–	–	–
8	W24 × 104	W14 × 145	W14 × 283	W18 × 46	W14 × 68	W14 × 132	–	–	–
9	W18 × 106	W14 × 109	W14 × 193	–	–	–	–	–	–
10	W18 × 86	W14 × 109	W14 × 193	–	–	–	–	–	–
11	W18 × 60	W14 × 53	W14 × 99	–	–	–	–	–	–
12	W18 × 35	W14 × 53	W14 × 99	–	–	–	–	–	–

Table 4 Calculations for the design of twelve-story frame with PBPD

	H_i (m)	m_i (ton)	$m_i H_i$	$\sum m_i H_i$	β_i	$\beta_i - \beta_{i+1}$	$(\beta_i - \beta_{i+1}) H_i$
Story 1	4.6	341.7	1571.8	106,892.0	3.78	0.04	0.175
Story 2	8.6	339	2915.4	105,320.2	3.75	0.07	0.610
Story 3	12.6	339	4271.4	102,404.8	3.68	0.11	1.325
Story 4	16.6	339	5627.4	98,133.4	3.57	0.14	2.337
Story 5	20.6	339	6983.4	92,506.0	3.43	0.18	3.679
Story 6	24.6	339	8339.4	85,522.6	3.25	0.22	5.399
Story 7	28.6	339	9695.4	77,183.2	3.03	0.26	7.577
Story 8	32.6	339	11,051.4	67,487.8	2.77	0.32	10.346
Story 9	36.6	339	12,407.4	56,436.4	2.45	0.38	13.950
Story 10	40.6	339	13,763.4	44,029.0	2.07	0.47	18.925
Story 11	44.6	339	15,119.4	30,265.6	1.60	0.60	26.870
Story 12	48.6	311.65	15,146.2	15,146.2	1	1	48.6
\sum	–	4043.35	106,892	–	34.38	3.785	139.79

Fig. 8 Elastic design spectrum

$$\alpha = 139.79 \left(\frac{15146.2}{106892} \right)^{0.75(1.618)^{-0.2}} \left(\frac{0.015 \times 8 \times \pi^2}{9.81 \times 1.618^2} \right) = 1.7027$$

The energy modification factor is also calculated as:

$$\gamma = \frac{2\mu_s - 1}{R_\mu^2} = \frac{2 \times 2.5 - 1}{2.5^2} = 0.64$$

Finally, the required design base shear is determined as:

$$\frac{V_y}{W} = \frac{-\alpha + \sqrt{\alpha^2 + 4\gamma S_a^2}}{2} = \frac{-1.7027 + \sqrt{1.7027^2 + 4 \times 0.64 \times 0.51^2}}{2} = 0.093$$

Design parameters of PBPD are reported in Table 5 for all archetype buildings. The design section of structural members based on the structural analysis is presented in Table 6.

The design process of other archetype buildings is similar to method presented for twelve-story frame that its results are shown in Table 6. To have an accurate assessment of the effectiveness of the design method, the sections of structural members should be selected such that difference between the required plastic modulus and the section plastic modulus is negligible. To this end, the interior columns of twelve-story frame designed using PBPD are W27. If these columns had been selected from W14 the same as the columns of twelve-story frame designed using DDBD, the section plastic modulus would have considerably more than the required plastic modulus that this may affect the effectiveness of design method. In order to be able to prove that the comparison of design methods has been performed in optimum situation of design, the required moment strength/moment capacity ratio is presented in Fig. 9. It can be found from this figure that this ratio is close or less than 1 and the design sections have been selected with high accuracy.

Table 5 Design parameters of PBPD

Design parameters	4-Story	8-Story	12-Story
T (s)	0.685	1.176	1.618
S_a (g)	1.204	0.702	0.510
θ_u	0.025	0.025	0.025
θ_y	0.01	0.01	0.01
θ_p	0.015	0.015	0.015
μ	2.5	2.5	2.5
R_μ	2.5	2.5	2.5
γ	0.64	0.64	0.64
α	3.329	2.167	1.703
V_y/W	0.259	0.137	0.093
V_b (MN)	3.379	3.604	3.676

5.3 Comparison of Design Parameters

In this section, a comparison between design parameters of DDBD and PBPD is performed. At the first place, difference in the ductility factor is found despite the same design objective. PBPD designed all archetype buildings with the ductility factor of 2.5, whereas DDBD has been assumed this factor equal to 2.56, 2.14 and 2.12 for four-, eight- and twelve-story buildings, respectively. Therefore DDBD assumes a lower ductility factor than PBPD in high-rise building, whereas this may be reversed in low-rise building.

Distribution shape of design base shear at the height of structure is presented in Fig. 10. This distribution shape is the ratio of seismic forces in each story to the top story. A significant difference is found between distribution shapes in DDBD and PBPD. This difference is also intensified with increasing the number of stories. Therefore, it can be con-

cluded that even if the design approaches of DDBD and PBPD result in the same design base shear, the designed structures will be different because of different distributions of base shear.

The comparison of design story shear can be found in Fig. 11. As shown in this figure, the design base shear of DDBD is less than that of PBPD in four-story archetype building, whereas in eight- and twelve-story archetype buildings, the design base shear of DDBD is more than that of PBPD. As instance in eight- and twelve-story archetype buildings, the design base shear of DDBD is almost 12.9% more than that of PBPD and in the four-story archetype building, the design base shear of DBDD is 15.9% less than that of PBPD. The design story shear of DDBD and PBPD is also completely different, especially in eight- and twelve-story archetype buildings as shown in Fig. 11. This is because of different distribution shapes defined in the design approaches of DDBD and PBPD as explained earlier.

The required moment strength of beams and columns is shown in Figs. 12 and 13. In four-story archetype buildings, the required moment strength of DDBD is less than that of PBPD. In high-rise buildings, PBPD leads to a larger required moment strength than DDBD in upper stories, whereas this is reversed in lower stories. Therefore, which of these design methods leads to a lighter high-rise building cannot be concluded. To find this, it is necessary to compare the required plastic modulus and weight of structural members.

The required plastic modulus of beams is shown in Fig. 14. DDBD approach obtains average of the required plastic modulus of beams at different stories equal to 3380, 4913 and 5102 cm³ in four, eight and twelve-story archetype buildings, respectively, whereas the corresponding values are 3956, 4513 and 4738 cm³ in PBPD approach. Therefore, it can be

Table 6 Archetype buildings designed by PBPD

Story	Twelve-story archetype building			Eight-story archetype building			Four-story archetype building		
	Beams	Exterior columns	Interior columns	Beams	Exterior columns	Interior columns	Beams	Exterior columns	Interior columns
1	W30 × 116	W14 × 193	W27 × 217	W30 × 116	W14 × 193	W14 × 370	W24 × 117	W14 × 176	W27 × 194
2	W30 × 116	W14 × 193	W27 × 217	W30 × 116	W14 × 193	W14 × 370	W24 × 103	W14 × 176	W27 × 194
3	W30 × 116	W14 × 211	W27 × 235	W30 × 108	W14 × 193	W14 × 370	W18 × 106	W14 × 159	W27 × 178
4	W30 × 116	W14 × 211	W27 × 235	W30 × 99	W14 × 193	W14 × 370	W18 × 71	W14 × 159	W27 × 178
5	W30 × 108	W14 × 211	W27 × 235	W30 × 90	W14 × 193	W14 × 342	–	–	–
6	W24 × 117	W14 × 211	W27 × 235	W27 × 84	W14 × 193	W14 × 342	–	–	–
7	W21 × 122	W14 × 193	W27 × 217	W18 × 86	W14 × 145	W14 × 257	–	–	–
8	W21 × 111	W14 × 193	W27 × 217	W18 × 60	W14 × 145	W14 × 257	–	–	–
9	W21 × 101	W14 × 176	W27 × 194	–	–	–	–	–	–
10	W18 × 97	W14 × 176	W27 × 194	–	–	–	–	–	–
11	W18 × 76	W14 × 120	W27 × 146	–	–	–	–	–	–
12	W18 × 50	W14 × 120	W27 × 146	–	–	–	–	–	–

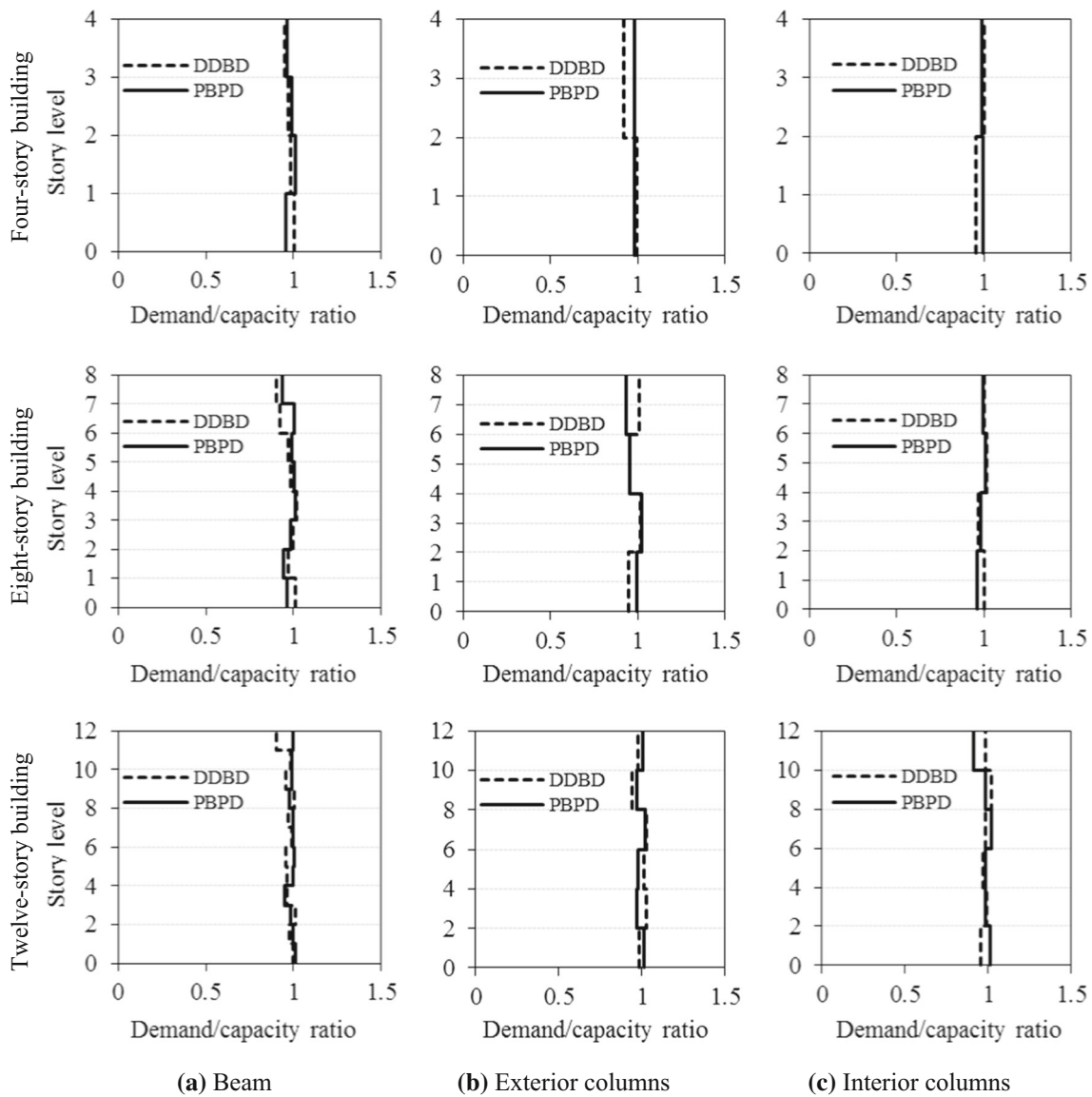


Fig. 9 Required moment strength/moment capacity ratio of design sections in DDBD and PBPD

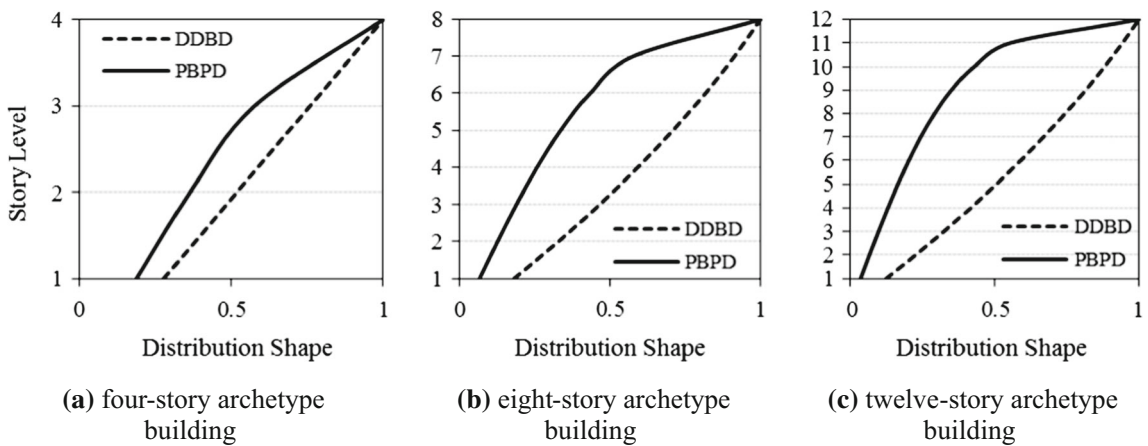


Fig. 10 Comparison of distribution shapes of design base shear defined in DDBD and PBPD (ratio of seismic forces in each story to the top story)

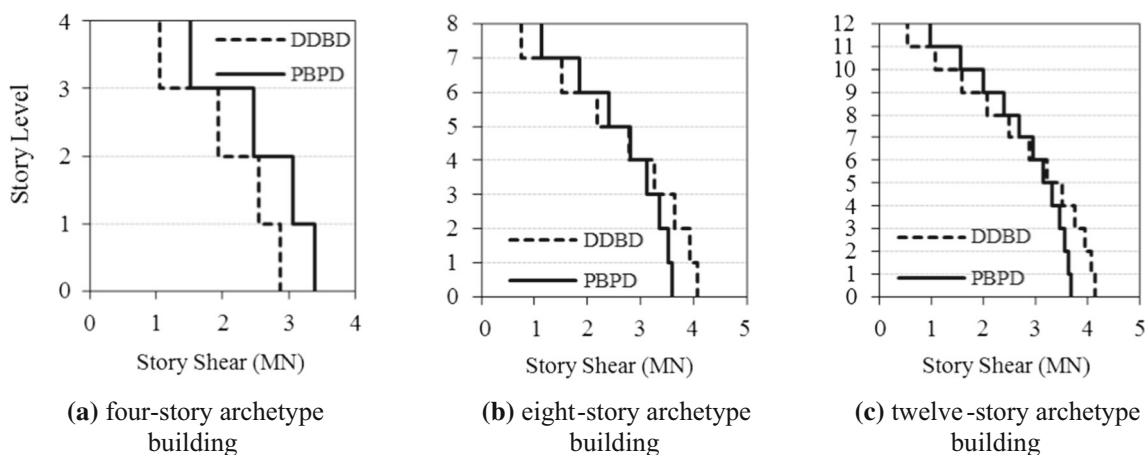


Fig. 11 Comparison of design story shears determined by DDBD and PBPD

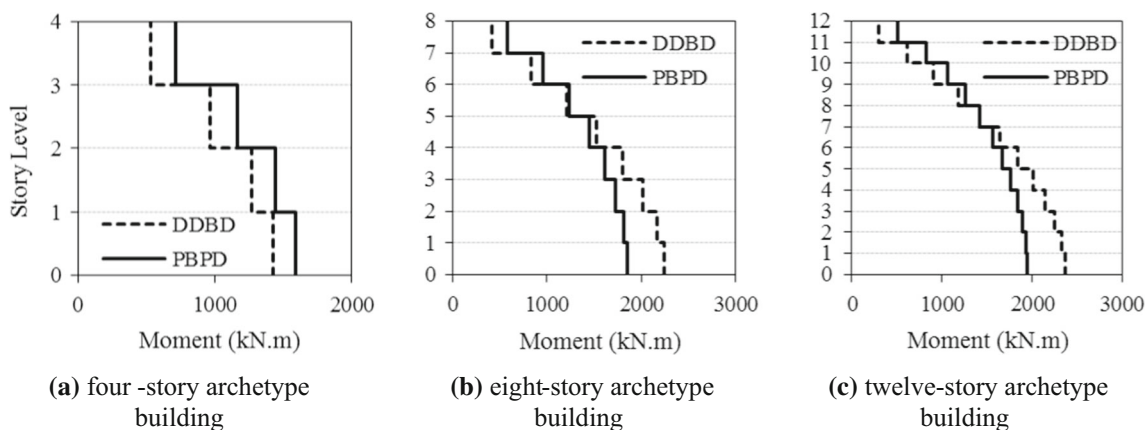


Fig. 12 Comparison of required moment strength of beams in DDBD and PBPD

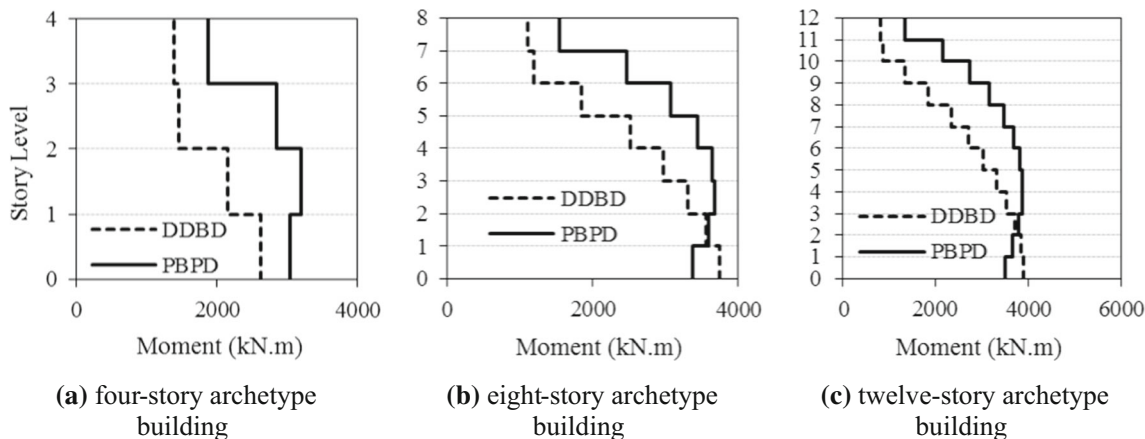


Fig. 13 Comparison of required moment strength of columns in DDBD and PBPD

concluded that DDBD designed the lighter and heavier beams in comparison with PBPD in low- and high-rise buildings, respectively. According to beam sections selected in previous section, it can be found that the total weight of beams designed by DDBD is almost 9.0, 22.0 and 34.6 ton in four-

eight- and twelve-story archetype buildings, respectively, whereas the corresponding values are 10.8, 20.7 and 33.9 ton in PBPD approach.

The required plastic modulus of interior columns is presented in Fig. 15. As shown in this figure, the required

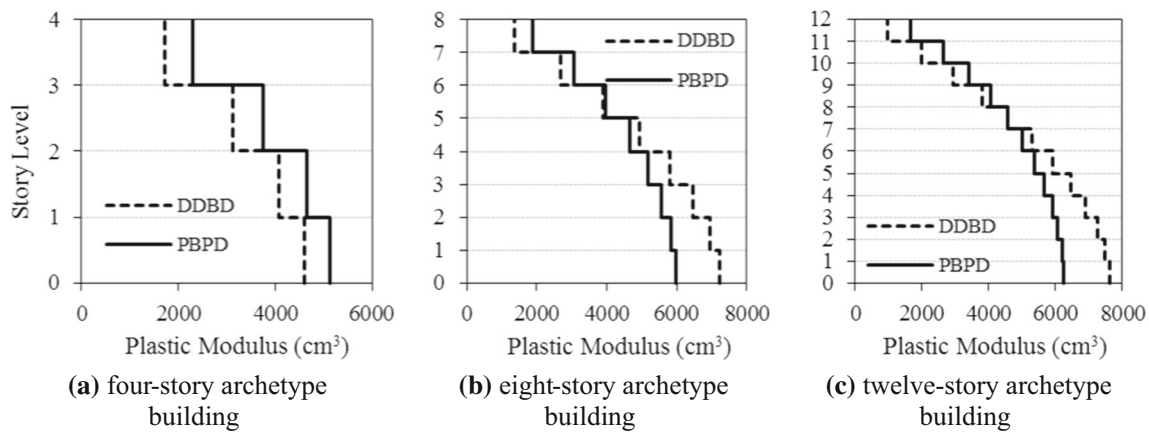


Fig. 14 Comparison of required plastic modulus of beams in DDBD and PBPD

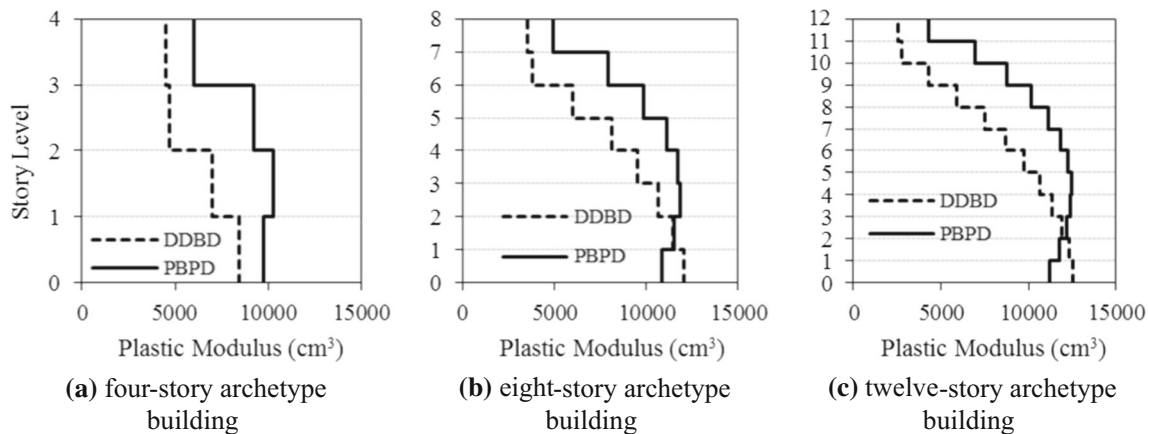


Fig. 15 Comparison of required plastic modulus of interior columns in DDBD and PBPD

plastic modulus of interior columns determined by PBPD is generally more than DDBD. Therefore, it can be concluded that the total weight of column sections designed by PBPD is more than DDBD. As instance in the eight-story frame, the total weight of columns designed in DDBD and PBPD approaches is 41.3 and 50.1 ton, respectively. The total weight of frame including beams and columns in DDBD and PBPD approaches is also 63.5 and 70.8 ton, respectively. Therefore, it can be concluded that DDBD leads to a lighter structure than PBPD.

6 Performance of Designed Archetype Buildings

In this section, the nonlinear time history analysis of deigned frames is performed under twenty-two earthquake records suggested by FEMA P695 [43] in order to identify more efficient design approach. These test earthquakes and their normalization factors are presented in Table 7. The normalized earthquake records must be scaled so that the median

value of spectrum acceleration of earthquake records is matched with the design spectrum at the fundamental period of structure. To this end, a scale factor is applied on the normalized earthquake records that these scaling factors are presented in Table 8. As instance, matching the median value of spectrum acceleration of earthquake records with the design spectrum is shown in Fig. 16 for four-story frame. Seismic performance of frames has been assessed using two-dimensional (2D) nonlinear models in Open System for Earthquake Engineering Simulation (OpenSees) [60]. The beams and columns are modeled using the nonlinear beam-column element with the fiber section. The kinematic material hardening of 3% is assumed to simulate the non-linearity of buildings. The nonlinear time history analysis is performed based on the Newmark- β method, while Rayleigh damping of 5% is applied at the first two modes of building. The maximum values of inter-story drift ratio are shown in Fig. 17. The average drift ratio and target drift limit have been also shown in this figure.

As shown in Fig. 17, although the drift ratio of four-story archetype buildings designed by DDBD and PBPD under

Table 7 Test earthquake records

ID No	Earthquake	Year	M	Station	PGA (g)	Normalization factor
1	Northridge	1994	6.7	Beverly Hills—Mulhol	0.52	0.651
2	Northridge	1994	6.7	Canyon Country-WLC	0.48	0.651
3	Duzce, Turkey	1999	7.1	Bolu	0.82	0.832
4	Hector Mine	1999	7.1	Hector	0.34	0.832
5	Imperial Valley	1979	6.5	Delta	0.35	0.629
6	Imperial Valley	1979	6.5	El Centro Array #11	0.38	0.629
7	Kobe, Japan	1995	6.9	Nishi-Akashi	0.5	1.092
8	Kobe, Japan	1995	6.9	Shin-Osaka	0.21	1.092
9	Kocaeli, Turkey	1999	7.5	Duzce	0.36	1.311
10	Kocaeli, Turkey	1999	7.5	Arcelik	0.15	1.311
11	Landers	1992	7.3	Yermo Fire Station	0.15	1.014
12	Landers	1992	7.3	Coolwater	0.42	1.014
13	Loma Prieta	1989	6.9	Capitola	0.44	1.034
14	Loma Prieta	1989	6.9	Gilroy Array #3	0.37	1.034
15	Manjil, Iran	1990	7.4	Abbar	0.5	1.099
16	Superstition Hills	1987	6.5	El Centro Imp. Co	0.26	1.099
17	Superstition Hills	1987	6.5	Poe Road (temp)	0.3	0.688
18	Cape Mendocino	1992	7.0	Rio Dell Overpass	0.55	0.688
19	Chi-Chi, Taiwan	1999	7.6	CHY101	0.44	1.360
20	Chi-Chi, Taiwan	1999	7.6	TCU045	0.51	1.360
21	San Fernando	1971	6.6	LA—Hollywood Stor	0.17	0.987
22	Friuli, Italy	1976	6.5	Tolmezzo	0.31	0.987

Table 8 Scale factor of earthquake records

		Four-story	Eight-story	Twelve-story
Period (s)	DDBD	1.38	2.18	3.28
	PBPD	1.17	2.19	3.19
Scale factor	DDBD	2.121	2.748	2.908
	PBPD	2.253	2.746	2.891

some earthquake records exceeds the target limit, the average value of drift ratios is less than the target limit. In eight-story archetype building, a slight exceedance of target drift limit can be found in the average drift ratio when the structure is designed using DDBD, whereas PBPD results in the average drift ratio less than the target limit. As instance, the maximum value of average drift ratio of eight-story archetype building designed using DDBD is 0.0264 that is 5.6% more than the drift limit. It can be found from Fig. 17 that the twelve-story archetype building designed using PBPD can be considered as a well-designed structure because the average drift ratio is less than the target limit, whereas the average drift ratio of structure designed using DDBD significantly exceeds the target limit. From Fig. 17a, the maximum value of average drift ratio is 0.0381 in twelve-story archetype

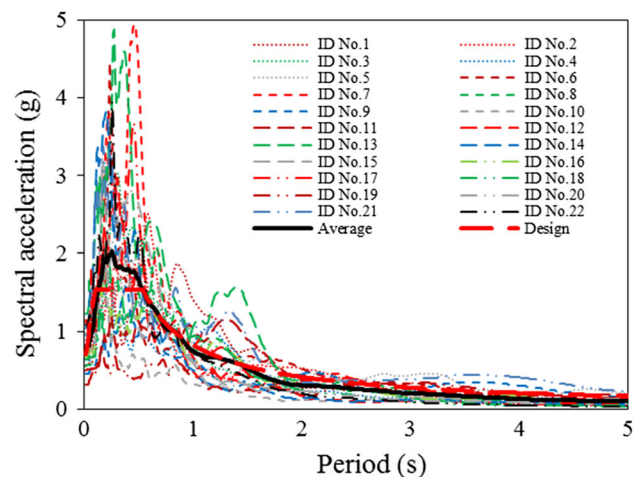


Fig. 16 Acceleration spectrum of scaled earthquake records for analysis of four-story frame designed by DDBD

building, while the design objective has been defined the achievement of drift ratio less than 0.025. According to the presented results, it can be concluded that in the low-rise steel moment frames, both DDBD and PBPD are efficient design approaches, whereas the effectiveness of DDBD approach is questioned by increasing the number of stories of structure.

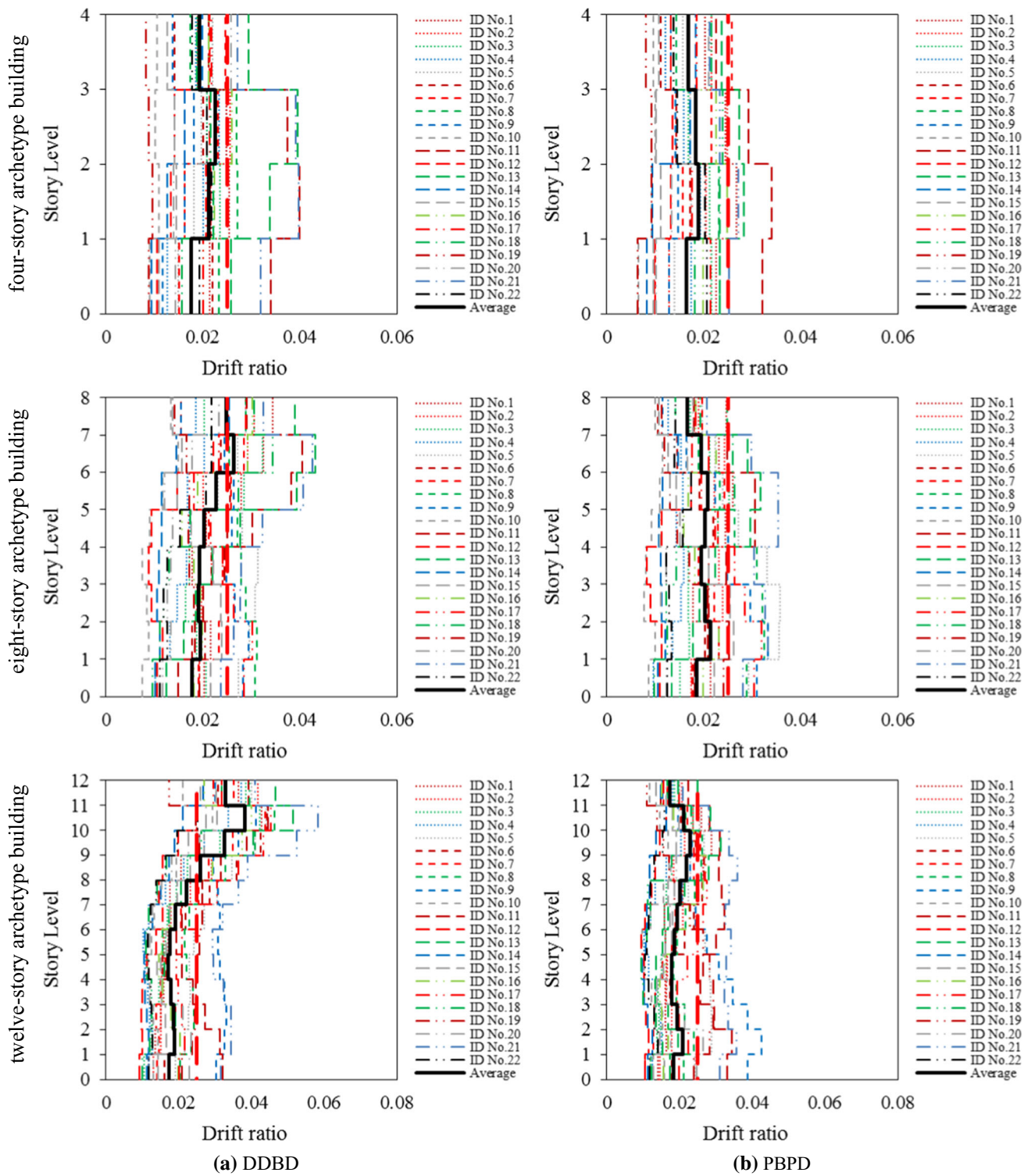


Fig. 17 Peak story drift ratio of archetype buildings designed by DDBD and PBPD

In this case study, PBPD approach generally is more effective than DDBD approach in the achievement of design objective.

The maximum values of story shear of archetype buildings are shown in Fig. 18 under test earthquake records. The

average story shear and the design story shear have been also presented in this figure. As shown, the average story shear is more than design shear in both design approaches. This can be due to different factors such as the strain hardening in the

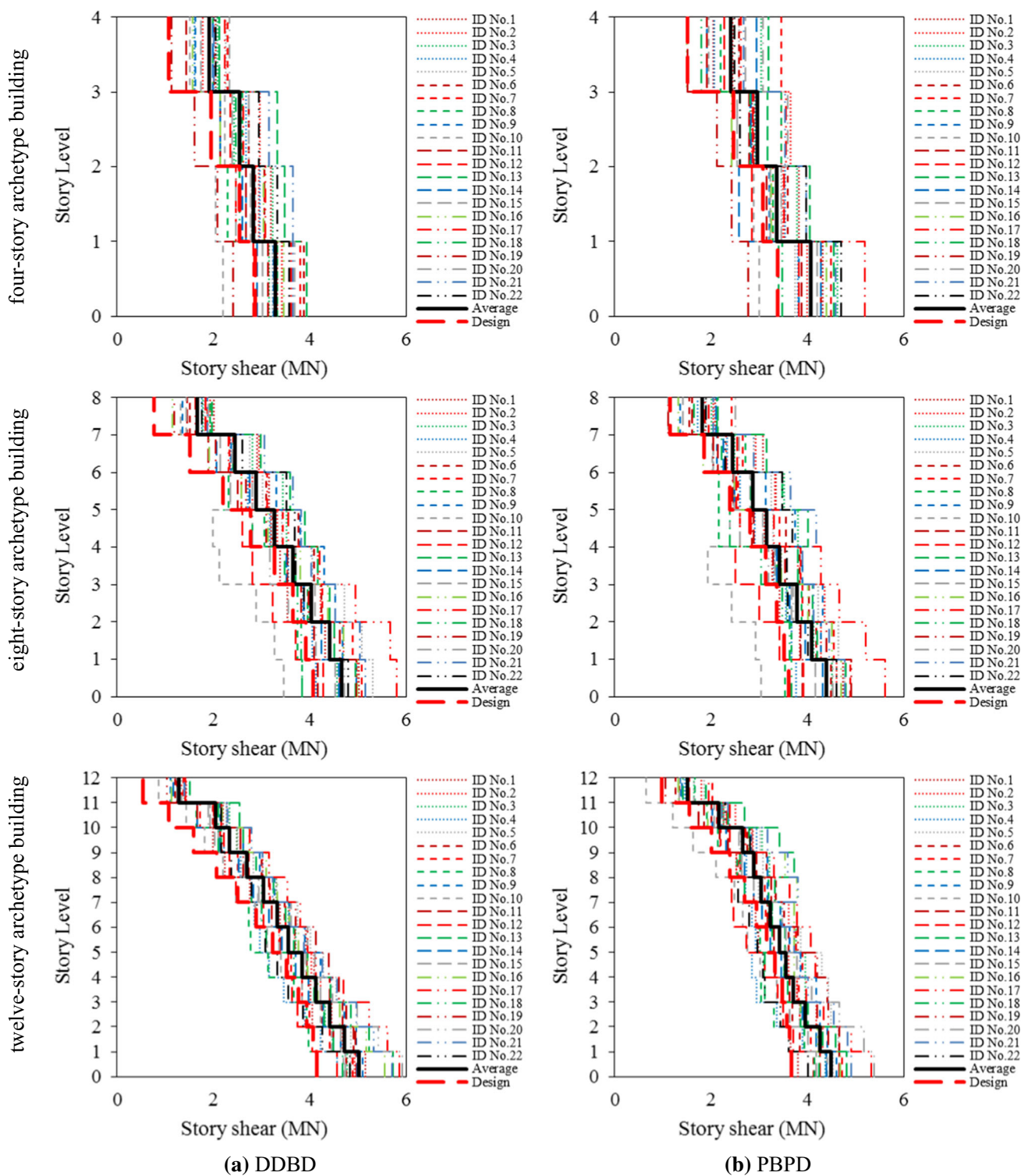


Fig. 18 Peak story shear of archetype buildings designed by DDBD and PBDP

elements and applying the strength-reduction factor in the design process of structural members. As instance, plastic hinges formed in archetype buildings are shown in Fig. 19 under earthquake record with ID No. 22.

It is noted that the desirable mechanism of moment frames is the formation of plastic hinges at beams and base columns. Figure 19a shows that DDBD leads formation of plastic hinges at columns except the base columns, whereas total

plastic hinges have been formed at the desirable locations in PBPD. Therefore the yield mechanism of buildings designed using DDBD may be undesirable, whereas PBPD effectively achieves the desirable yield mechanism. It must be noted that the design base shear of DDBD was more than that of PBPD, so the increase of design base shear will be unreasonable to solve this drawback because the required strength of structural members in lower stories will be too much. Different methods can be proposed to solve this drawback and improve the effectiveness of DDBD in future studies as follows:

- (1) DDBD leads formation of plastic hinges at columns of upper stories. This undesirable performance in upper stories is because of its distribution function, and the modification of distribution model can be effective to improve the effectiveness of DDBD approach [61].
- (2) The aim of this study is to compare DDBD and PBPD, so the design process of DDBD was implemented exactly as proposed in Priestley et al. [3]. The columns were designed by applying two coefficients of φ^o and ω on the required design moment of beams. The design of columns based on the moment capacity of beams and the weak beam–strong column principle can be desired to prevent the formation of plastic hinges in columns.
- (3) The increase in the coefficient of ω related to upper stories can strengthen the columns of these stories and solve the drawback of plastic hinges.

7 Conclusion

In this study, a comparison has been conducted between direct displacement-based design (DDBD) and performance-based plastic design (PBPD) to identify more efficient design approach. To this end, three steel moment-resisting frames with different heights of 4, 8 and 12 stories have been designed using DDBD and PBPD to achieve life safety performances level under seismic hazard having a probability of occurrence 10% in 50 years. Significant difference can be found between the design parameters of these design approaches. DDBD obtains lower and higher design base shear than PBPD in low- and high-rise buildings, respectively. As instance, DDBD has determined the design base shears of four- and twelve-story buildings equal to 2.86 MN and 4.15 MN, respectively, whereas the corresponding values are 3.38 MN and 3.68 MN in PBPD. Although DDBD obtains higher design base shear in comparison with PBPD in high-rise buildings, DDBD leads to a lighter structure than PBPD. This is because of significant difference of these design approaches in the design base shear distribution at the height of structure. As instance in eight-story frame, the total weight of moment-resisting frames designed

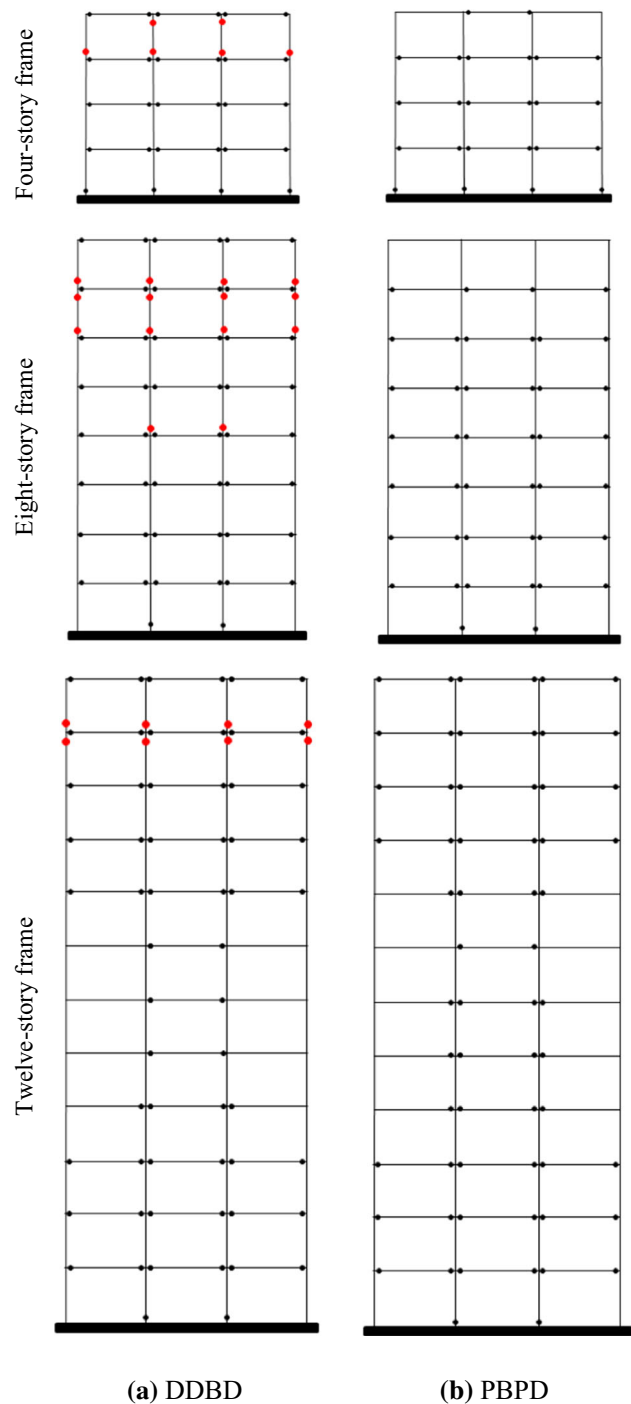


Fig. 19 Location of plastic hinges under earthquake record with ID No. 22

using DDBD and PBPD approaches is 63.5 and 70.8 ton, respectively. DDBD approach distributes the base shear such that the design story shear at upper stories is significantly lower. Because of this distribution model, DDBD leads formation of plastic hinges at columns of upper stories, whereas total plastic hinges have been formed at the desirable locations in PBPD. To validate the achievement of design

performance level, nonlinear time history analysis of steel moment-resisting frames has been performed under twenty-two earthquake records. The results show that both DDBD and PBPD have achieved the desirable performance level in low-rise steel moment frames, whereas the effectiveness of DDBD approach is questioned by increasing the number of stories of structure. As instance, the maximum value of average drift ratio is 0.0381 in twelve-story archetype building designed using DDBD, whereas the design objective has been defined the achievement of drift ratio less than 0.025. PBPD has effective performance even in high-rise building. As instance, the maximum value of average drift ratio is 0.023 in twelve-story archetype building designed using PBPD. Therefore in this case study, PBPD approach is generally more effective than DDBD approach for steel moment-resisting frames.

References

- ASCE 7–10: Minimum design loads for buildings and other structures. American Society of Civil Engineers, Reston VA, (2010)
- Priestley, M.N.: Myths and fallacies in earthquake engineering. *Bull. N. Z. Soc. Earthq. Eng.* **26**(3), 329–341 (1993)
- Priestley, M.N.; Calvi, G.M.; Kowalsky, M.J.: Displacement-based seismic design of structures. IUSS press, Pavia, Italy (2007)
- FEMA 356: Prestandard and commentary for the seismic rehabilitation of buildings. American Society of Civil Engineers, Washington DC, (2000)
- Krawinkler, H.; Miranda, E.: Performance-based earthquake engineering. CRC Press, Boca Raton, FL (2004)
- FEMA P-58: Seismic performance assessment of buildings: volume 1-methodology. Applied Technology Council for the Federal Emergency Management Agency, Washington DC, (2012)
- O'Reilly, G.J.; Calvi, G.M.: Conceptual seismic design in performance-based earthquake engineering. *Earthq. Eng. Struct. Dyn.* **48**(4), 389–411 (2019)
- Shahnazaryan, D.; O'Reilly, G.J.: Integrating expected loss and collapse risk in performance-based seismic design of structures. *Bull. Earthq. Eng.* **19**(2), 987–1025 (2021)
- Aschheim, M.; Black, E.F.: Yield point spectra for seismic design and rehabilitation. *Earthq. Spectra* **16**(2), 317–335 (2000)
- Englekirk, R.E.: Seismic Design of Reinforced and Precast Concrete Buildings. John Wiley & Sons, Hoboken, NJ (2003)
- Sullivan, T.; Priestley, M.; Calvi, G.M.: A Model Code for the Displacement-Based Seismic Design of Structures DBD12. IUSS Press, Pavia, Italy (2012)
- Shibata, A.; Sozen, M.A.: Substitute-structure method for seismic design in R/C. *J. Struct. Div.* **102**, 1–18 (1976)
- Sullivan, T.J.: Highlighting differences between force-based and displacement-based design solutions for reinforced concrete frame structures. *Struct. Eng. Int.* **23**(2), 122–131 (2013)
- Priestley, M.; Kowalsky, M.: Direct displacement-based seismic design of concrete buildings. *Bull. N. Z. Soc. Earthq. Eng.* **33**(4), 421–444 (2000)
- Yan, L.; Gong, J.: Development of displacement profiles for direct displacement based seismic design of regular reinforced concrete frame structures. *Eng. Struct.* **190**, 223–237 (2019)
- Muho, E.V.; Qian, J.; Beskos, D.E.: A direct displacement-based seismic design method using a MDOF equivalent system: application to R/C framed structures. *Bull. Earthq. Eng.* **18**, 4157–4188 (2020)
- Medhekar, M.; Kennedy, D.: Displacement-based seismic design of buildings—theory. *Eng. Struct.* **22**(3), 201–209 (2000)
- Wijesundara, K.; Nascimbene, R.; Sullivan, T.: Equivalent viscous damping for steel concentrically braced frame structures. *Bull. Earthq. Eng.* **9**(5), 1535–1558 (2011)
- Grande, E.; Rasulo, A.: Seismic assessment of concentric X-braced steel frames. *Eng. Struct.* **49**, 983–995 (2013)
- Sahoo, D.R.; Prakash, A.: Seismic behavior of concentrically braced frames designed using direct displacement-based method. *Int. J. Steel Struct.* **19**(1), 96–109 (2019)
- Sullivan, T.J.: Direct displacement-based seismic design of steel eccentrically braced frame structures. *Bull. Earthq. Eng.* **11**(6), 2197–2231 (2013)
- O'Reilly, G.J.; Sullivan, T.J.: Direct displacement-based seismic design of eccentrically braced steel frames. *J. Earthq. Eng.* **20**(2), 243–278 (2016)
- Fakhraddini, A.; Hamed, S.; Fadaee, M.J.: Peak displacement patterns for the performance-based seismic design of steel eccentrically braced frames. *Earthq. Eng. Eng. Vib.* **18**(2), 379–393 (2019)
- Sullivan, T.; Maley, T.; Calvi, G.: Seismic response of steel moment resisting frames designed using a Direct DBD procedure. In: Proceedings of the 8th International Conference on Structural Dynamics, Leuven, Belgium, 2011
- Roldán, R.; Sullivan, T.; Della Corte, G.: Displacement-based design of steel moment resisting frames with partially-restrained beam-to-column joints. *Bull. Earthq. Eng.* **14**(4), 1017–1046 (2016)
- Cardone, D.; Palermo, G.; Dolce, M.: Direct displacement-based design of buildings with different seismic isolation systems. *J. Earthq. Eng.* **14**(2), 163–191 (2010)
- Ye, K.; Xiao, Y.; Hu, L.: A direct displacement-based design procedure for base-isolated building structures with lead rubber bearings (LRBs). *Eng. Struct.* **197**, 109402 (2019)
- Moradpour, S.; Dehestani, M.: Optimal DDBD procedure for designing steel structures with nonlinear fluid viscous dampers. *Structures* **22**, 154–174 (2019)
- Noruzvand, M.; Mohebbi, M.; Shakeri, K.: Modified direct displacement-based design approach for structures equipped with fluid viscous damper. *Struct. Control Health Monit.* **27**(1), e2465 (2020)
- O'Reilly, G.J.; Calvi, G.M.: Quantifying seismic risk in structures via simplified demand–intensity models. *Bull. Earthq. Eng.* **18**(5), 2003–2022 (2020)
- Malekpour, S.; Ghaffarzadeh, H.; Dashti, F.: Direct displacement-based design of steel-braced reinforced concrete frames. *Struct. Des. Tall Spec.* **22**(18), 1422–1438 (2013)
- Leelataviwat, S.; Goel, S.C.; Stojadinović, B.: Toward performance-based seismic design of structures. *Earthq. Spectra* **15**(3), 435–461 (1999)
- Lee, S.-S.; Goel, S.C.; Chao, S.-H.: Performance-based seismic design of steel moment frames using target drift and yield mechanism. In: Proceedings of the 13th World Conference on Earthquake Engineering, Vancouver, Canada, 2004
- Dasgupta, P.; Goel, S.C.; Parra-Montesinos, G.; Tsai, T.: Performance-based seismic design and behavior of a composite buckling restrained braced frame. In: Proceedings of the 13th World Conference on Earthquake Engineering, Vancouver, BC, 2004
- Housner, G.W.: The plastic failure of structures during earthquakes. In: Proceedings of Second World Conference on Earthquake Engineering, Tokyo, Japan, 1960
- Banihashemi, M.R.; Mirzagoltabar, A.; Tavakoli, H.: Development of the performance based plastic design for steel moment resistant frame. *Int. J. Steel Struct.* **15**(1), 51–62 (2015)



37. Ganjavi, B.; Gholamrezatabar, A.; Hajirasouliha, I.: Effects of soil-structure interaction and lateral design load pattern on performance-based plastic design of steel moment resisting frames. *Struct. Des. Tall Spec.* **28**(11), e1624 (2019)
38. Ghamari, M.; Shoostari, M.: Application of performance-based plastic design (PBSD) method for 3D steel structures. *Eng. Struct.* **199**, 109649 (2019)
39. Chao, S.-H.; Goel, S.C.: Performance-based seismic design of EBF using target drift and yield mechanism as performance criteria. University of Michigan, Ann Arbor, MI (2005)
40. Banihashemi, M.; Mirzagoltabar, A.; Tavakoli, H.: Reliability and fragility curve assessment of steel concentrically braced frames. *Eur. J. Environ. Civ. Eng.* **20**(7), 748–770 (2016)
41. Sahoo, D.R.; Chao, S.-H.: Performance-based plastic design method for buckling-restrained braced frames. *Eng. Struct.* **32**(9), 2950–2958 (2010)
42. Chao, S.; Goel, S.: Performance-based plastic design of seismic resistant special truss moment frames (STMF). University of Michigan, Ann Arbor, MI (2006)
43. FEMA P695: Quantification of Building Seismic Performance Factors. American Society of Civil Engineers, Washington DC, (2009)
44. Vision 2000: Performance Based Seismic Engineering of Buildings. Structural Engineers Association of California, California, (1995)
45. Sullivan, T.; Lago, A.: Towards a simplified direct DBD procedure for the seismic design of moment resisting frames with viscous dampers. *Eng. Struct.* **35**, 140–148 (2012)
46. Pettinga, J.D.; Priestley, M.N.: Dynamic behaviour of reinforced concrete frames designed with direct displacement-based design. *J. Earthq. Eng.* **9**(2), 309–330 (2005)
47. Rosenblueth, E.; Herrera, I.: On a kind of hysteretic damping. *J. Eng. Mech. Div.* **90**(4), 37–48 (1964)
48. Miranda, E.; Ruiz-García, J.: Evaluation of approximate methods to estimate maximum inelastic displacement demands. *Earthq. Eng. Struct. Dyn.* **31**(3), 539–560 (2002)
49. Grant, D.N.; Blandon, C.; Priestley, M.: Modelling Inelastic Response in Direct Displacement-Based Design. European School of Advanced Studies in Reduction of Seismic Risk, Pavia, Italy, (2005)
50. Dwairi, H.M.; Kowalsky, M.J.; Nau, J.M.: Equivalent damping in support of direct displacement-based design. *J. Earthq. Eng.* **11**(4), 512–530 (2007)
51. Newmark, N.M.; Hall, W.J.: *Earthquake Spectra and Design*. Earthquake Engineering Research Institute, Berkeley, CA, (1982)
52. Priestley, M.: *Myths and Fallacies in Earthquake Engineering*. IUSS press, Pavia, Italy (2003)
53. EN 1998–1: Eurocode 8: Design of structures for earthquake resistance-part 1: general rules, seismic actions and rules for buildings. European Committee for Standardization, Brussels, Belgium, (2004)
54. Güneş, E.M.; D’Aniello, M.; Landolfo, R.; Mermerdaş, K.: Prediction of the flexural overstrength factor for steel beams using artificial neural network. *Steel Compos. Struct.* **17**(3), 215–236 (2014)
55. AISC 341–10: Seismic provisions for structural steel buildings. American Institute of Steel Construction, Chicago, IL, (2010)
56. Chao, S.-H.; Goel, S.C.; Lee, S.-S.: A seismic design lateral force distribution based on inelastic state of structures. *Earthq. Spectra* **23**(3), 547–569 (2007)
57. Goel, S.C.; Chao, S.H.: Performance-based plastic design: earthquake-resistant steel structures. International Code Council, Washington DC (2008)
58. Zareian, F.; Lignos, D.; Krawinkler, H.: Evaluation of seismic collapse performance of steel special moment resisting frames using FEMA P695 (ATC-63) methodology. In: Structures Congress 2010, Orlando, Florida, (2010)
59. Elkady, A.; Lignos, D.G.: Effect of gravity framing on the overstrength and collapse capacity of steel frame buildings with perimeter special moment frames. *Earthq. Eng. Struct. Dyn.* **44**(8), 1289–1307 (2015)
60. Mazzoni, S.; McKenna, F.; Scott, M.H.; Fenves, G.L.: *OpenSees command language manual*. University of California, Berkeley, CA (2006)
61. Shakeri, K.; Dadkhah, H.: Development of DDBD for steel MRFs using inelastic response-based seismic lateral force distribution. *J. Build. Eng.* **43**, 103063 (2021)

